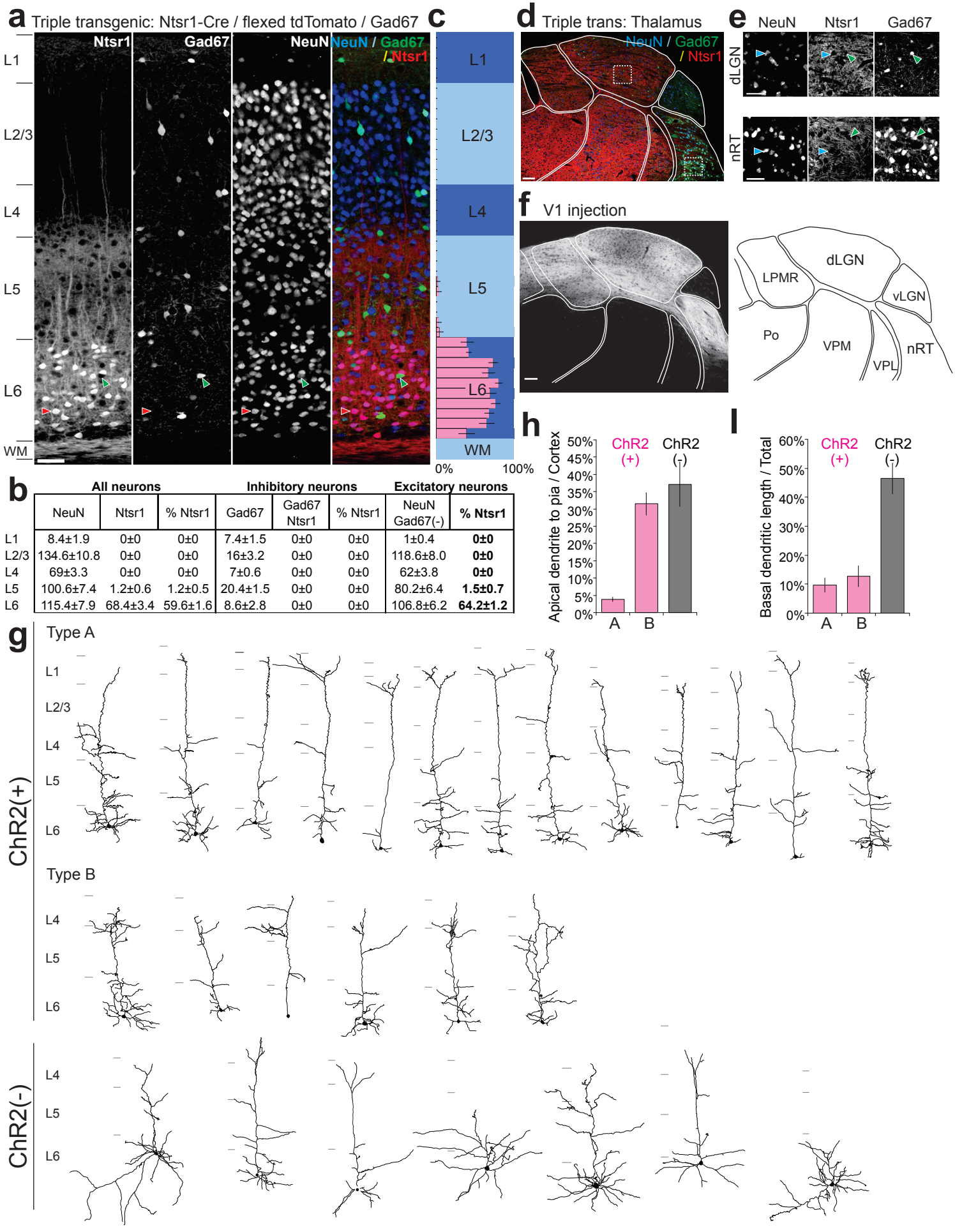

b

	All neurons			Inhibitory neurons			Excitatory neurons	
	NeuN	Ntsr1	% Ntsr1	Gad67	Gad67 Ntsr1	% Ntsr1	NeuN Gad67(-)	% Ntsr1
L1	8.4±1.9	0±0	0±0	7.4±1.5	0±0	0±0	1±0.4	**0±0**
L2/3	134.6±10.8	0±0	0±0	16±3.2	0±0	0±0	118.6±8.0	**0±0**
L4	69±3.3	0±0	0±0	7±0.6	0±0	0±0	62±3.8	**0±0**
L5	100.6±7.4	1.2±0.6	1.2±0.5	20.4±1.5	0±0	0±0	80.2±6.4	**1.5±0.7**
L6	115.4±7.9	68.4±3.4	59.6±1.6	8.6±2.8	0±0	0±0	106.8±6.2	**64.2±1.2**

Supplemental Figure 1. Histological and morphological characterization of the NTSR1-Cre line.

Supplemental Figure 1. Histological and morphological characterization of the NTSR1-Cre line.

a. Confocal section of V1 from triple transgenic mouse (NTSR1-Cre x floxed-tdTomato reporter x Gad67-GFP). NeuN is a neuronal marker. Red arrowheads indicate NTSR1 expressing neuron in all color channels. Green arrowheads indicate Gad67 expressing interneuron. Scale bar: 50 μm.
b. Summary of stereological counts from V1 of triple transgenic mouse (shown in (a)). Counts were done in a 200 μm wide box drawn across all cortical layers and averaged over 5 sections (Bregma -2.7 to -2.9) from the same mouse. Note that all NTSR1 positive cells expressed NeuN and no NTSR1 cells expressed Gad67.
c. Summary histogram of percentage of NTSR1 expressing excitatory neurons across layers (n = 5 sections; same as (b)).
d. Coronal section of thalamus (Bregma -2) of same triple transgenic shown in (a). Scale bar: 50 μm. Boundaries of different nuclei are traced in white (see (f) for legend).
e. Zoom in of boxed areas in (d). Note that NTRS1 does not label cell bodies (NeuN) in dLGN (top row) or nRT (bottom row). Scale bar: 25 μm.
f. Left: NTSR1-Cre mouse injected in V1 with AAV transducing flexed tdTomato. Note that the projection pattern of dTomato expressing L6 axon is restricted to the dLGN, nRT and LPMR. Boundaries of different nuclei are traced in white (see right panel for legend). Right: Schematic of boundaries of thalamic nuclei (determined by Franklin and Paxinos, 2008). dLGN: dorsal lateral geniculate nucleus; LPMR: LP thalamic nuclei, medial rostral; nRT: thalamic reticular nucleus; Po: posterior thalamic nuclear group; vLGN: ventral lateral geniculate nucleus; VPM: ventral posteromedial thalamic nuclei.
g. Reconstructions of biocytin filled L6 neurons from NTRS1-Cre mice previously injected with AAV transducing floxed-tdTomato ChR2. Only the dendrites are shown. Expression of ChR2 was determined by the spiking of the neurons (recorded in the cell attached configuration) in response to a brief (2ms) pulse of LED and confirmed by the photocurrent elicited in the whole cell voltage clamp configuration. All ChR2(+) neurons could be subdivided into two categories: those whose apical dendrite reached L1 (Type A) and those whose apical dendrite ended at L4 (Type B). Neurons whose primary apical dendrite exited the slice plane are not shown and were not quantified.
h. Summary histogram of the distance from apical dendrite to the pia normalized by the radial extent of the cortical section for the two ChR2(+) and the ChR2(-) groups of neurons shown in (g).
i. Summary histogram of the total length of basal dendrites, normalized to the total dendritic length (apical and basal) for the three groups shown in (g).

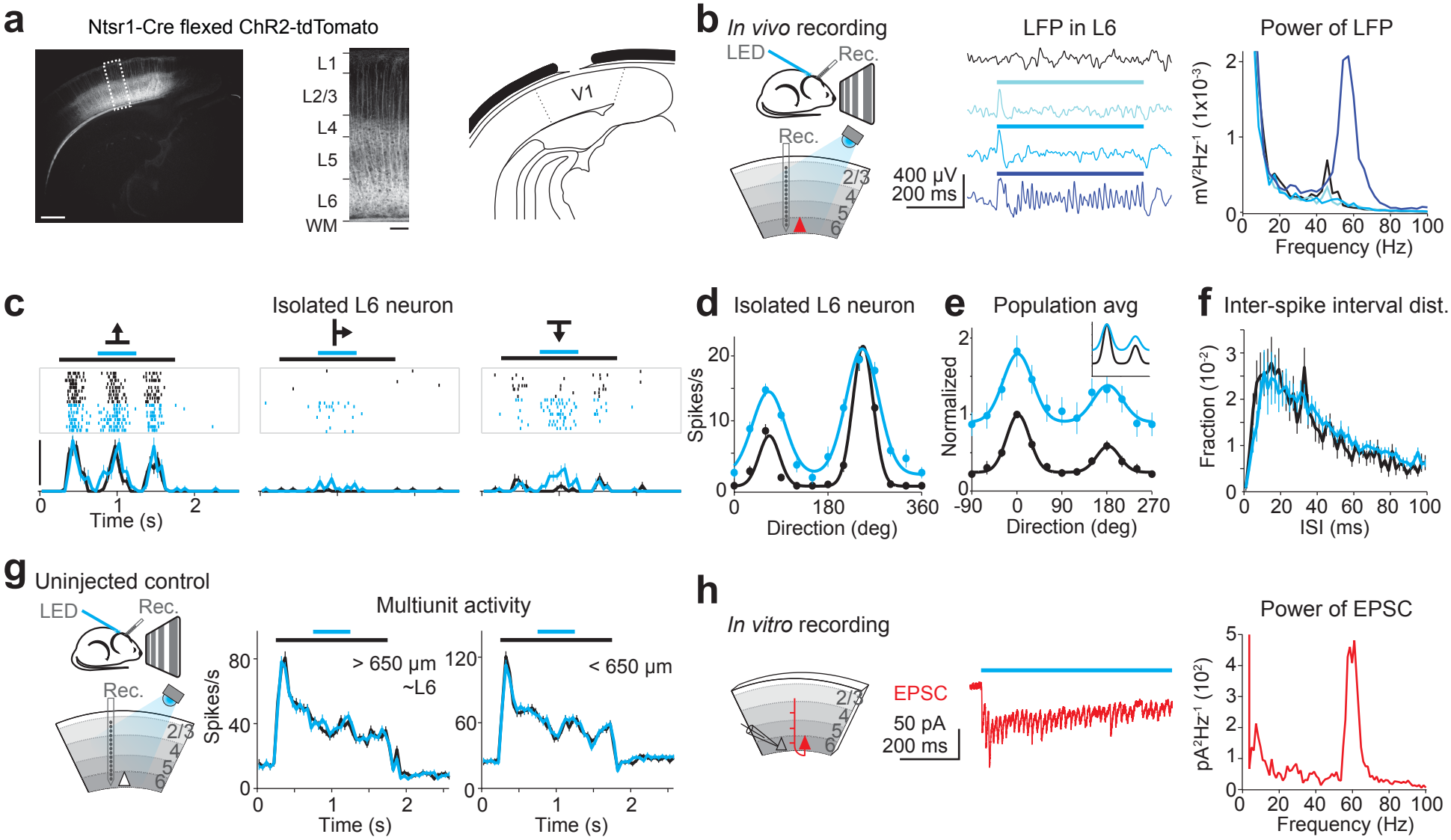

Supplemental Figure 2. Characterization of L6 photo-stimulation.

Supplemental Figure 2. Characterization of L6 photo-stimulation.

a. Left, coronal section showing expression of flexed-ChR2-tdTomato in V1 (scale bar, 500 μm). Middle, higher magnification of region shown in box (scale bar, 100 μm). Right, schematic of coronal slice and method for restricting LED illumation to center of V1. Entire skull except ~1-2 mm region in center of V1 is covered with black cement to block LED from illuminating regions outside of V1. Skull overlying V1 is thinned and small craniotomy is made for insertion of probe.
b. Left, schematic of *in vivo* recording setup and L6 photo-stimulation. Center, local field potential (bandpass filtered, 1-100 Hz) recorded in L6 under control conditions (black) or with increasing LED levels. LED intensities increase from light blue to purple and correspond to the 2nd, 3rd, and highest intensities shown in Fig. 1. All LED intensities shown here are sufficient to suppress visually evoked cortical activity (Fig. 1). he strongest intensity also generates oscillations at gamma frequency, consistent with previous observations (Adesnik and Scanziani, 2010). Horizontal bar indicates duration of LED illumination. Right, power spectrum of LFP traces. Note that gamma frequency (~60Hz) is generated only by the highest LED intensity (purple trace), indicating that gamma oscillations are not necessary for L6 mediated suppression of cortical activity.
c. Response of isolated putative ChR2-expressing L6 cell to visual stimuli of different orientations (3 of 12 tested directions are shown) under control (black) or during photo-stimulation (blue). Top: raster plots; Bottom: PSTH. Scale bar, 50 spikes/s. Horizontal black and blue bars show duration of visual stimulus and of LED illumination, respectively.
d. Tuning curve for control trials (black) and trials with photo-stimulation (blue).
e. Population tuning curves for ChR2-expressing L6 neurons under control (black) and photo-stimulation (blue) (n = 19). The LED intensity was the same as for Fig. 2a-e. On average, photo-stimulation adds a similar number of spikes to the control responses. This offset broadens the tuning of photo-stimulated L6 neurons (mean change in OSI -0.18±0.03 ($p < 10^{-5}$). Inset, tuning curves normalized separately for control and photo-stimulation conditions.
f. Average normalized histogram (2 ms bins) of inter-spike intervals for putative ChR2-expressing L6 cells under control (black) and photo-stimulation (blue) conditions. Note that photo-stimulation using this LED intensity does not dramatically alter L6 neuron spike statistics.
g. Left: schematic of *in vivo* recording setup for visual stimulation and LED illumination in a NTSR1-Cre mouse that has not been injected with the ChR2 expressing virus. Middle, PSTH of multiunit activity recorded in L6 with (blue) and without (black) LED illumination. Right, PSTH of multiunit activity recorded in upper layers. Horizontal black and blue bars show duration of visual stimulus and of LED illumination, respectively.
h. Left, *in vitro* recording setup. Middle, response of a ChR2-negative L6 pyramidal cell to photo-stimulation of L6 (cell was voltage clamped at reversal potential for inhibition). The oscillations in the excitatory postsynaptic current (EPSC) have a similar frequency to those generated *in vivo* with the highest LED intensity (see (b)). Horizontal bar indicates duration of LED illumination. Right, power spectrum of current trace.

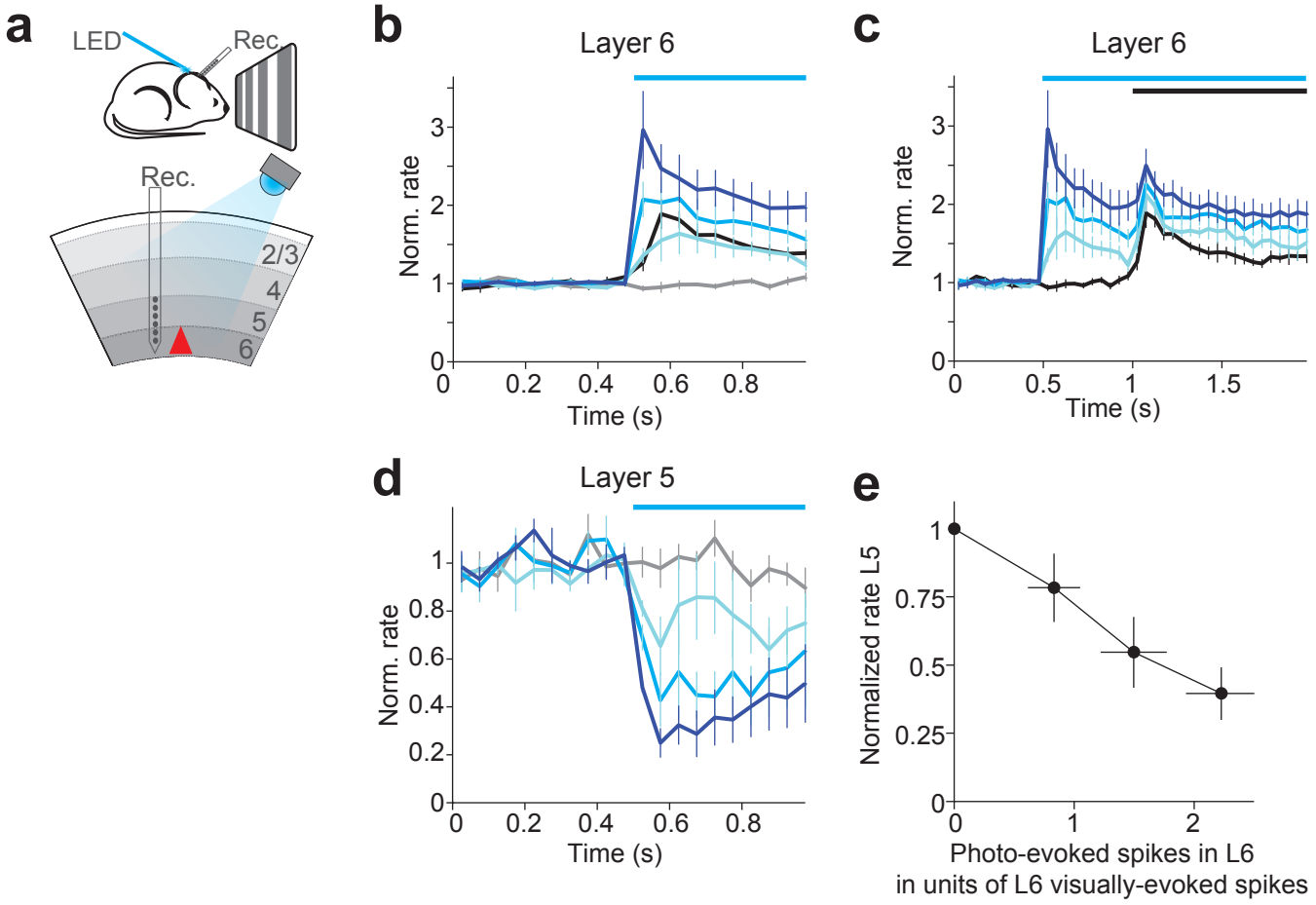

Supplemental Figure 3. Photo-stimulation of L6 to physiological rates suppresses spontaneous cortical activity.

a. Schematic of *in vivo* recording setup and L6 photo-stimulation.

b. Activity rates produced by photo-stimulation are within the range elicited by visual stimulation. PSTHs show normalized multiunit activity in L6 elicited with either photo-stimulation (blue colors) or visual stimulation (black) (n = 5 penetrations across 3 mice; the same experiments are illustrated in the rest of the figure). Darker blue colors indicate higher LED intensity (these LED intensities correspond to the three lowest intensities in Fig. 1, and encompass the intensities used for Fig. 2a-c.). Blue horizontal bar shows LED illumination (applicable to the blue PSTHs) or visual stimulation (applicable to the black PSTH). Gray PSTH shows activity in absence of both LED and visual stimulus. Note that photo-stimulation evokes L6 activity that is within the range evoked by visual stimulation and that these L6 activity levels are sufficient to suppress visually evoked activity (Fig. 1) and spontaneous activity (see(d) in other layers.

c. Control experiment demonstrating that photo-stimulation of L6 does not saturate the L6 response range. L6 was photo-stimulated prior to the visual stimulus. PSTHs show that photo-stimulation does not prevent L6 neurons from responding to visual stimulus, indicating that their activity is not forced to a ceiling by the photo-stimulation. PSTH coloring is the same as in b. Black bar indicates visual stimulus and blue bar indicates LED illumination.

d. Photo-stimulation of L6 in the absence of a visual stimulus suppresses spontaneous multiunit activity in L5. PSTH coloring is the same as in b. Blue bar indicates LED illumination.

e. Suppression of spontaneous activity in L5 as a function of activity produced by photo-stimulation of L6. L6 activity is quantified in terms of the number of spikes produced by photo-stimulation relative to the visual stimulus over the 500 ms duration of the LED.

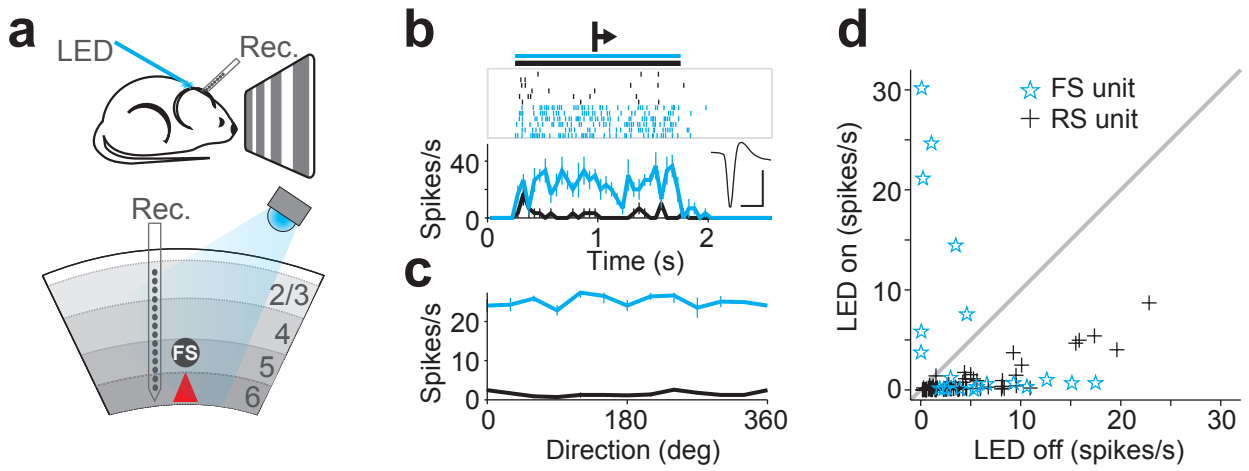

Supplemental Figure 4. The only cortical cells indirectly activated by L6 photo-stimulation are fast spiking (FS) units.

a. Schematic showing setup for recording visual responses while photo-stimulating L6. The activity of a fast spiking putative inhibitory neuron is recorded during photo-stimulation of ChR2-expressing L6 pyramidal neurons.
b. Raster and PSTH showing activation of an FS cell during visual stimulation without (black) or with (blue) L6 photo-stimulation. Inset, average spike waveform (Scale bars: 200 µV, 0.5 ms).
c. Tuning curve for control trials (black) and trials with L6 photo-stimulation (blue).
d. Scatter plot showing all units recorded in cortex with and without L6 photo-stimulation (n = 90). Regular spiking and FS cells are indicated by the plus and star symbols, respectively. Seven out of 19 FS cells were significanlty activated by L6 photo-stimulation. Notice that the only units above the unity line (gray) are FS units.

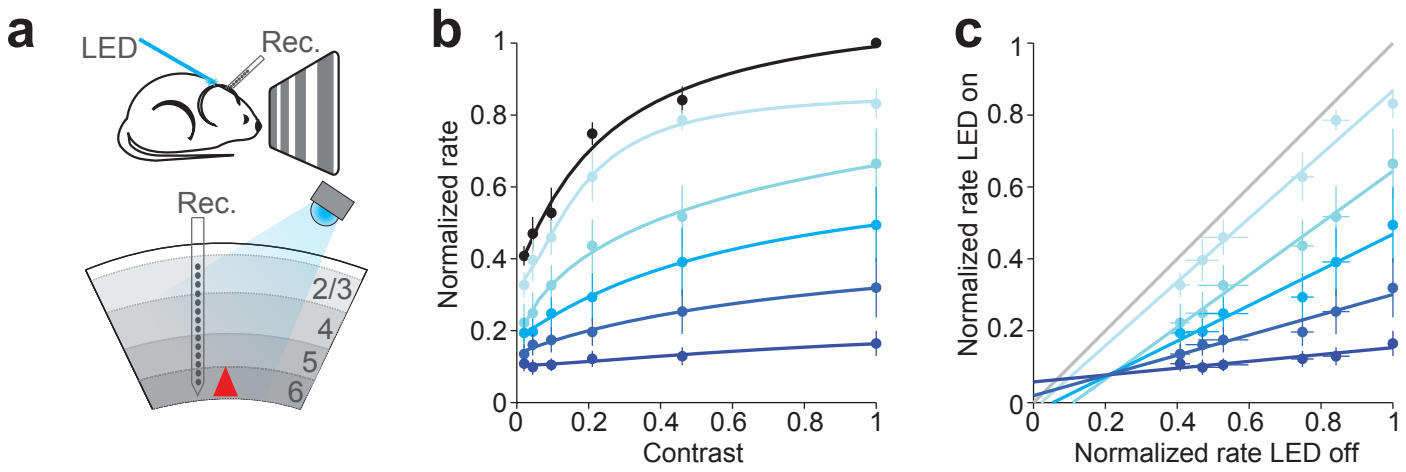

Supplemental Figure 5. V1 contrast response functions with L6 photo-stimulation.

a. Schematic showing setup for recording visual responses while photo-stimulating L6.
b. Average normalized V1 multiunit contrast response functions with increasing levels of L6 photo-stimulation (n = 5). Multiunit activity was pooled across L2-L5. Control (no LED) is shown in black. Progressively stronger LED intensities are represented by lighter to darker colors.
c. Normalized activity under control conditions (x-axis) against activity with photo-stimulation of L6 (y-axis). Blue lines are linear fits; gray line is unity.

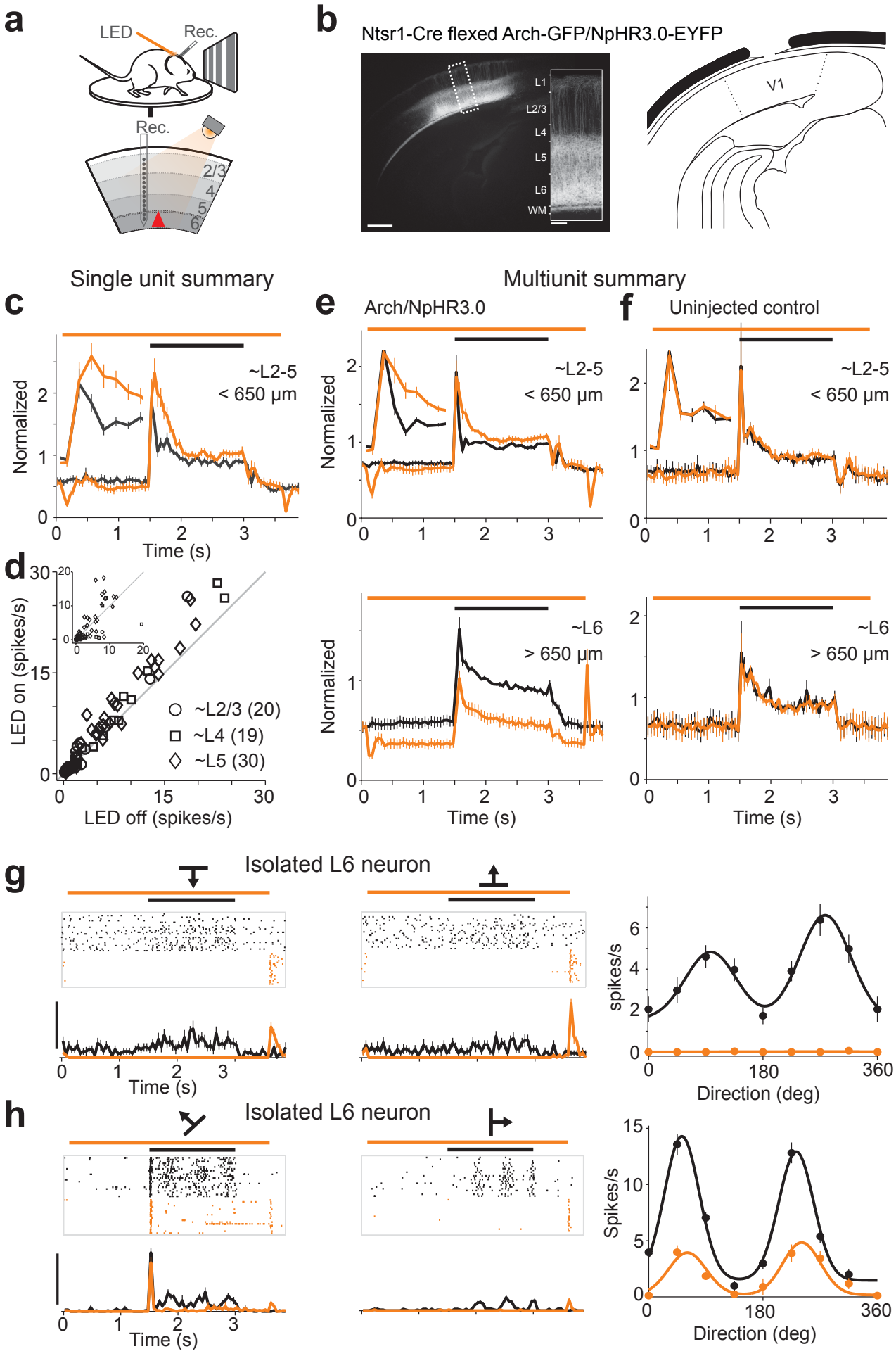

Supplemental Figure 6. Photo-suppression of L6 facilitates other layers in awake mice.

Supplemental Figure 6. Photo-suppression of L6 facilitates other layers in awake mice.

a. Schematic of setup for recording, visual stimulation and L6 photo-suppression in awake head-fixed mouse running on circular treadmill.
b. Left, coronal section showing expression of flexed-Arch-GFP and flexed-NpHR3.0-EYFP in V1 (scale bar, 500 μm). Inset, higher magnification of region shown in box (scale bar, 100 μm). Right, schematic of coronal slice and method for restricting LED illumation to center of V1.
c. Average PSTH of visually evoked activity in all isolated units in L2-5 under control (black) or during L6 photo-suppression (orange). Inset, onset of the resonse to visual stimulation on an expanded timescale. The onset of the LED preceded the visual stimulus by 1.4 s. While baseline activity was transiently decreased at onset of LED consistently across units, the sustained effect on baseline activity was variable (see inset in (d)).
d. Response of all isolated units with and without photo-suppression of L6 (n values are shown in parentheses). Each symbol is the average response of one unit. On average responses were facilitated by 24±10% ($p = 0.026$), 10±4% ($p = 0.023$), 30±10% ($p = 0.004$, $n = 30$) in L2/3, L4, and L5, respectively. Two L5 units had rates above 30 Hz and are not shown on graph. Inset, effect of L6 photo-suppression on baseline activity (firing rate computed in 1s window prior to visual stimulus).
e. PSTH of visually evoked multiunit activity under control (black) or during L6 photo-suppression (orange). Note that activity is suppressed in L6 (bottom; $p<10^{-5}$, $n = 7$) but facilitated in L2-5 (top; $p = 10^{-6}$, $n = 7$). PSTH is normalized to mean activity occurring during visual stimulation under control condition. Horizontal black and orange bars show duration of visual stimulus and of LED illumination, respectively. Inset, onset of the resonse to visual stimulation on an expanded timescale.
f. As in (c) but in an NTSR1-Cre mouse that was not injected with Arch or NpHR3.0 expressing virus. Note the lack of effect of LED illumination on visually evoked activity in L6 (bottom, $p = 0.40$, $n = 4$) and L2-5 (top; $p = 0.59$, $n = 4$).
g. Example L6 neuron that is completely suppressed by LED illumination. Right, tuning curves with (orange) and without LED (black).
h. Example L6 neuron that is incompletely suppressed by LED illumination. Tuning is similar despite reduction in firing rate.

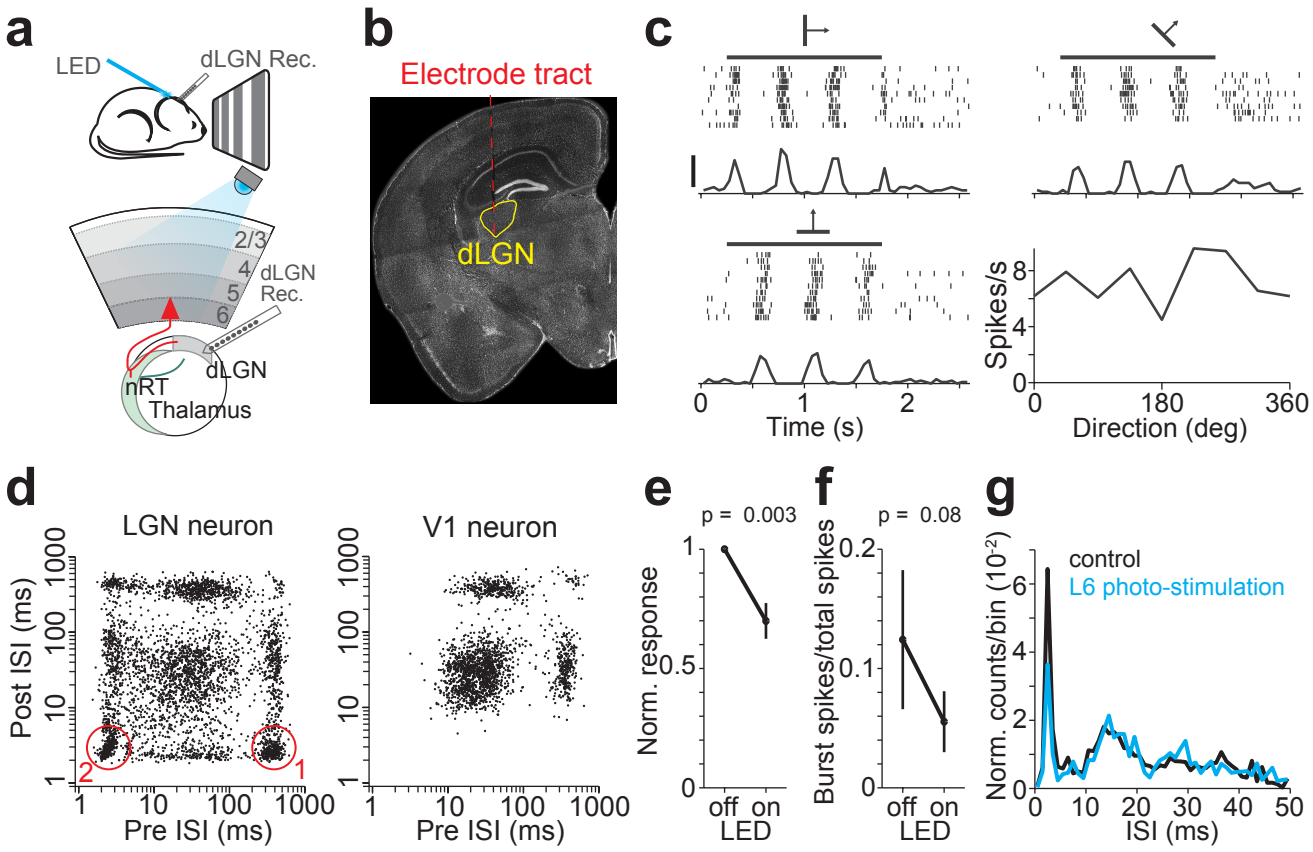

Supplemental Figure 7. Recording visual responses in dLGN.

a. Schematic of *in vivo* setup for recording visual responses in dLGN.

b. Coronal section of Dapi-stained brain in which a recording was made from dLGN with a linear multichannel probe. Electrode tract confirms correct targeting of dLGN.

c. Rasters and PSTHs show response of isolated dLGN unit to drifting gratings of different orientations. Note the phasic nature of firing (occurring at the temporal frequency of stimulus, 2Hz). Bottom-right, tuning curve for the unit in (c). Note the lack of tuning for orientation.

d. The inter-spike interval (ISI) preceding a spike (pre ISI) is plotted against the ISI following a spike for two example isolated units recorded in dLGN (top) and V1 (bottom). The plots illustrate the different firing pattern of dLGN and V1 neurons and highlight the presence of spike bursts, characteristic of dLGN neurons (encircled clusters on the left plot). Cluster 1 includes spikes that were preceded by a long ISI (> 200 ms), but then were followed by a second spike within 2-4 ms; these represent the first spike in a burst. Cluster 2 shows spikes that were both preceded and followed by a short ISI; these are middle spikes in a burst.

e. Average normalized response of 11 isolated dLGN units tested with a moderate level of L6 photo-stimulation leading to an average 30±8% reduction in visually evoked firing rate. These units were used for the analysis in parts f and g.

f. Fraction of visually evoked dLGN spikes occurring in a burst during control (LED off) or L6 photo-stimulation (LED on). Burst spikes are defined as those spikes preceded by an inter-spike inteval (ISI) ≥100 ms and followed by an ISI of ≤ 4 ms; subsequent spikes occurring with an ISI ≤ 4 ms are considered part of the burst. L6 photo-stimulation leads to a small and non-significant decrease in the fraction of burst spikes.

g. Normalized histogram of ISI values under control (black) or during L6 photo-stimulation (blue). Note the overlapping distribution of ISIs in control versus photo-stimulation.

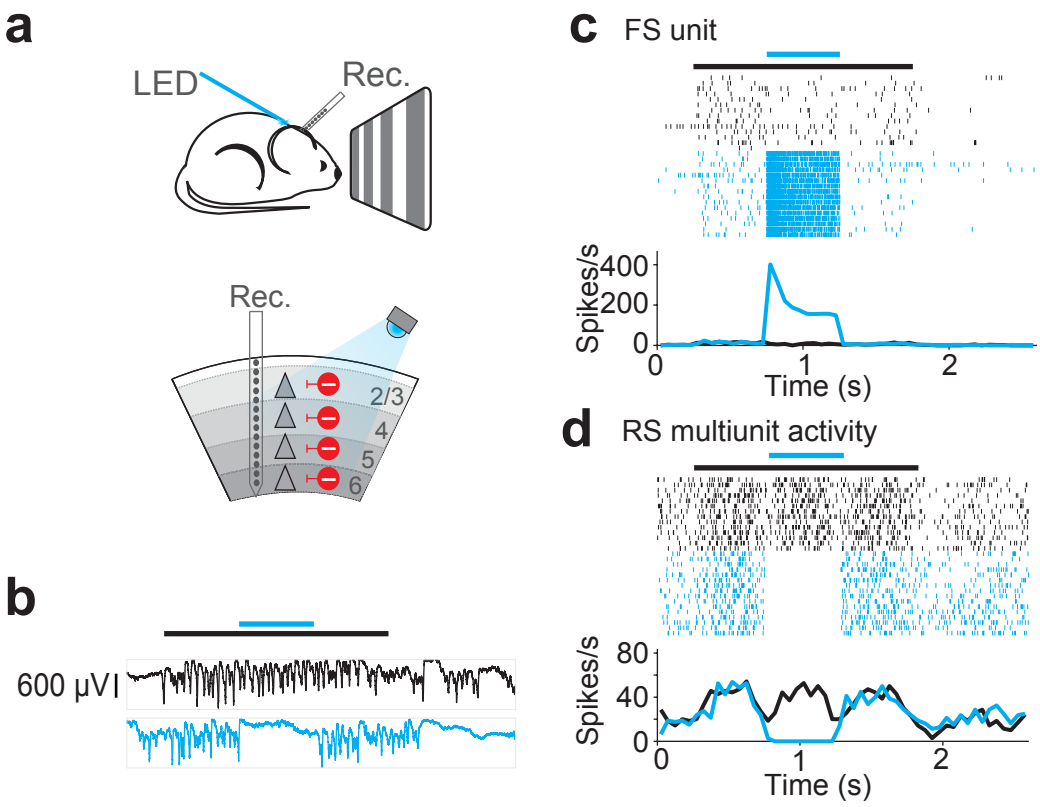

Supplemental Figure 8. Method for rapidly and completely silencing V1 using optogenetics.

a. Schematic showing setup for recording visual evoked activity in V1 while photo-stimulating parvalbumin-expressing (PV) inhibitory neurons.

b. Example local field potential recorded in V1 without (black) and with photo-stimulation (blue) of PV neurons. The LFP generated by the visual stimulus (black horizontal bar, 1.5 s) is completely and reversibly suppressed when photo-stimulating PV neurons (blue bar, 500 ms).

c. Raster plot (top) and PSTH (bottom) of fast spiking (FS, putative PV+ neuron; see methods) unit recorded in V1 without (black) and with (blue) photo-stimulation of PV neurons. Horizontal black and blue bars show duration of visual stimulus and of LED illumination, respectively. Note that the unit is strongly driven by the LED.

d. Regular spiking multiunit activity recorded in V1 in response to visual stimulation without (black) or with photo-stimulation (blue) of PV neurons. Horizontal black and blue bars show duration of visual stimulus and of LED illumination, respectively. Note the complete and reversible suppression of visually evoked activity.

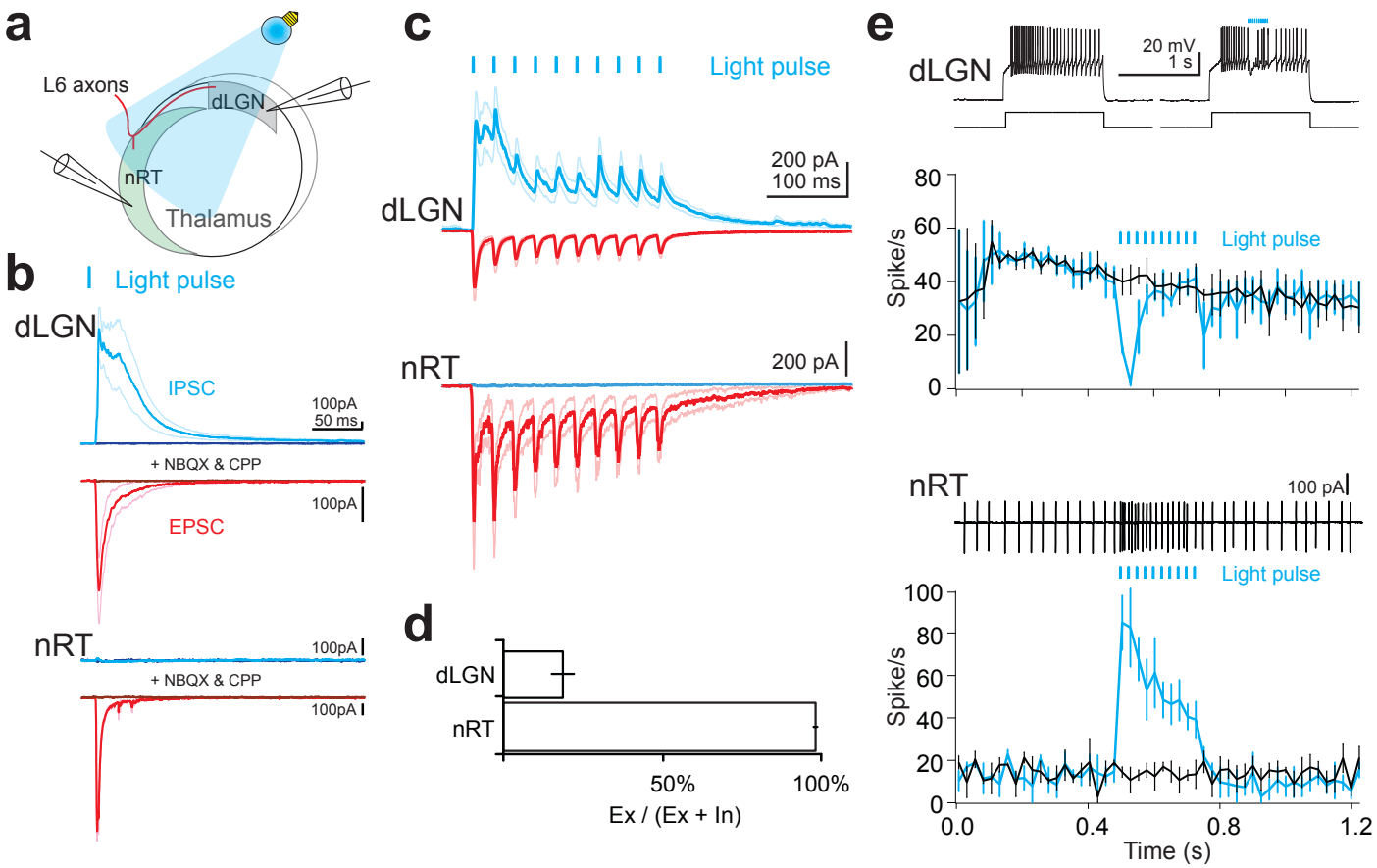

Supplemental Figure 9. Photo-stimulation of L6 axons recruits strong disynaptic inhibition in the dLGN but only monosynaptic excitation in the nRT.

a. Schematic of setup for whole cell recordings in thalamic slice during photo-stimulation of severed layer 6 axons. Entire thalamus was illuminated with the LED.

b. Average IPSCs (blue) and EPSCs (red) recorded in neurons voltage clamped at the reversal potential for EPSCs and IPSCs, respectively during single-pulse (2ms; vertical blue line) photo-stimulation of L6 axons. Note different scale bar for different traces. Light blue and red traces show SEM. Top: Both IPSCs and EPSCs recorded in the dLGN (averages of 3 different whole cell recordings) are abolished by the perfusion of the AMPA and NMDA receptor antagonists NBQX (10 µM) and CPP (20 µM), respectively (darker traces), indicating that IPSCs were of disynaptic origin. Bottom: The EPSC recorded in the nRT (average of 5 traces from the same neuron) is also abolished upon perfusion of NBQX and CPP. Note the nRT did not receive inhibition.

c. As in (b) but in response to multi-pulse photo-stimulation of L6 axons delivered at 40 Hz. The synaptic currents recorded in the dLGN and the nRT are the averages of 9 and 5 different whole cell recordings, respectively. Previous studies have shown that L6 inputs to the thalamus are facilitating, but here we observe synaptic depression during the photo-stimulation train. This is probably because 1. ChR2 desensitizes after each stimulus, and 2. direct, strong axonal photo-stimulation (as is necessary in thalamic slices, where the somatodendritic compartment of L6 neurons is absent) leads to an increase in release probability (as compared to a normal action potential), and thus a decrease in synaptic facilitation (Schoenberger et al. Exp. Physiol 2011).

d. Summary histogram of excitatory charge from recordings shown in (c) as a percentage of total charge.

e. Top traces: perforated patch current clamp recording from dLGN relay neuron in response to depolarizing current injection (1 every 30s) alternated between control conditions (left) and 40 Hz photo-stimulation of L6 axons (right). Blue dashes show LED illumination. Top graph: PSTH of spike rate in control (black) and with photo-stimulation of L6 axons (blue; n= 4). Bottom traces: cell attached recording showing spontaneous firing of nRT neuron and response to 40 Hz photo-stimulation of L6 axons. Bottom graph: PSTH of spike rate before and after photo-stimulation of L6 axons, black and blue respectively (n=3). Time scale for recording is the same as for PSTH. Note that dLGN neurons decrease their evoked firing rate upon photo-stimulation of L6 axons, while the spontaneous firing rate of the nRT neurons is facilitated.

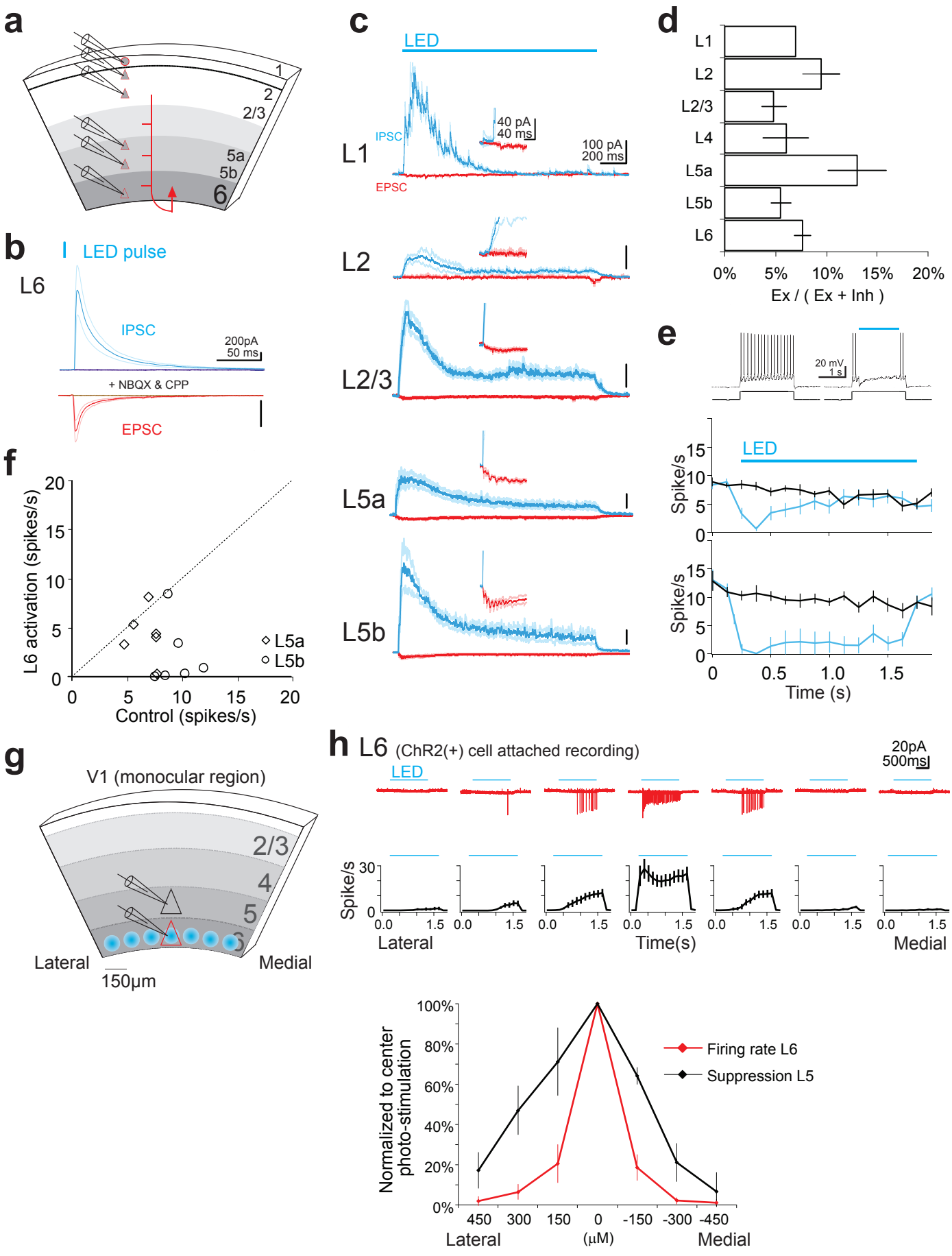

Supplemental Figure 10. Sub-layer specific differences in intra-cortical inhibition in response to of L6 photo-stimulation.

Supplemental Figure 10. Sub-layer specific differences in intra-cortical inhibition in response to of L6 photo-stimulation.

a. Schematic of setup for whole cell recordings in V1 slice during L6 photo-stimulation.
b. Average IPSCs (blue) and EPSCs (red) recorded in ChR2(-) L6 pyramidal cells voltage clamped at the reversal potential for EPSCs and IPSCs, respectively, during photo-stimulation (2 ms pulse, horizontal blue line) of L6. The synaptic currents recorded are the average of 3 different whole cell recordings. Both IPSCs and EPSCs are abolished by the addition of the AMPA and NMDA receptor antagonists NBQX (10 μM) and CPP (20 μM), respectively (darker traces), indicating that IPSCs were of disynaptic origin.
c. L1, L2, L2/3, L5a and L5b neurons voltage clamped at the reversal potential for EPSCs and IPSCs, respectively, during photo-stimulation of L6. The synaptic currents recorded in layers 1, 2, 2/3, 5a and 5b are the averages of 1, 2, 9, 6 and 6, different whole cell recordings, respectively. Inset shows onset of EPSC. Horizontal blue bar show duration of LED illumination. All recorded L2 pyramidal cells bordered L1. L2 pyramidal cells were not included in the L2/3 population. L2/3 data (from Fig. 4c) are included for comparison. All recorded L5a pyramidal cells were located below L4 and above the sub-layer formed by large pyramidal cells. All recorded L5b neurons were the large pyramidal cells located above L6. L5 in figure 4c is an average of these L5a and L5b recordings.
d. Summary histogram showing excitatory charge from recordings shown in (c) as a percentage of total charge. L4 and L6 data (from Fig. 4c) are included for comparison.
e. Top traces: perforated patch current clamp recording from L5b pyramidal cell in response to depolarizing current injection (1 every 30s) alternated between control conditions (left) and photo-stimulation of L6 (right). Horizontal blue bar shows duration of LED illumination. Bottom graphs: PSTH of spike rate in control (black) and with photo-stimulation of L6 (blue; L5a: n= 6; L5b: n= 6). L5 in figure 4e is an average of these two populations. Note that photo-stimulation of L6 suppresses firing rate in L5b to a greater extent and for a longer duration than in L5a, consistent with the larger contribution of the excitatory charge to the total charge recorded in L5a pyramidal cells, and shown in (d).
f. Average spike rate of individual cells from (e) plotted against the spike rate with L6 photo-stimulation. Same L5 data points shown in figure 4e but separated in L5a and L5b.
g. Spatially confined activation of ChR2(+) L6 pyramidal cells by focal photo-stimulation. Left: Schematic of recording configuration. Right: Direct activation of ChR2(+) L6 pyramidal cell in the cell-attached mode by a circular photo-stimulus. Example traces of light-evoked spikes recorded in the cell-attached configuration of a of ChR2(+) L6 pyramidal cell as the focal photo-stimulus was translated laterally across L6 in 150 μm steps (top) and PSTH for each photo-stimulus location (bottom).
h. Average spatial profile of light evoked firing across ChR2(+) L6 pyramidal cells (red; n = 8). The spatial profile of L5 pyramidal cell suppression (black; from Fig 4h) is superimposed, for comparison.